

Gantry Crane Model for Control System

November 15, 2019

Dustin Gurley
Bradley Long
Wyatt McKibbin
Derek Beck

ES205 Analysis and Design of Engineering Systems
Prof. Layton



Introduction

The gantry crane system is an apparatus composed of a crane with a free-swinging pendulum attached. The crane moves freely along a track parallel to the ground and is driven by a DC motor via a set of pulleys and a screw shaft. The system is similar to cranes that maneuver shipping containers. When moving the shipping containers, there should be very little sway of the container, because this could affect the contents of the container and pose a safety hazard. There are systems in place that help reduce the sway of the containers while also maneuvering them at an efficient pace.

The goal of this experiment is to develop a transfer function to allow a control design team to design a controller that minimizes the sway of the load. By shifting the crane at the right time at the right speed, the pendulum oscillation may be counteracted and dampened. We achieve this goal by creating a mathematical model that simulates the position of the pendulum over time.

Apparatus

The experimental setup is shown in figure 6. The system consists of several different subsystems. The overall system starts with a controller that outputs a voltage through leads to a DC motor. The voltage causes the DC motor to spin, which then spins the drive gears. This causes the bottom pulley to spin. The 3 identical pulleys are connected by belts linking their rotations together. The rotation of the top pulley drives the rotation of the lead screw which moves along a fixed horizontal bar. As the lead screw moves horizontally, it moves a crane fixed to a different horizontal bar. The crane slides along this bar on wheels. There is a pendulum attached to the crane that swings freely with a load attached near the bottom.

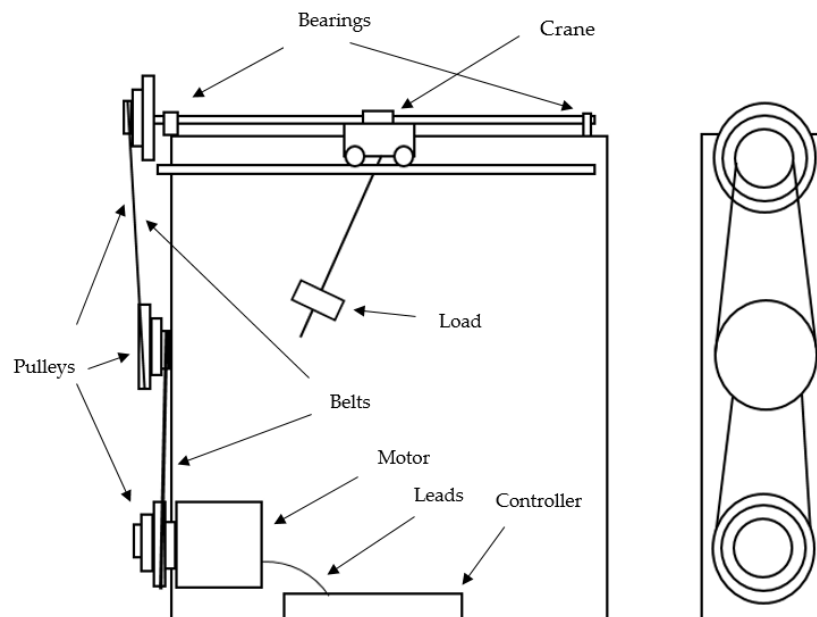


Figure 1: Crane and load system with drive apparatus, front (left) and side (right)

Model

For the first system, we model the motor as a resistor, an inductor and a back emf voltage source as seen in figure 2.

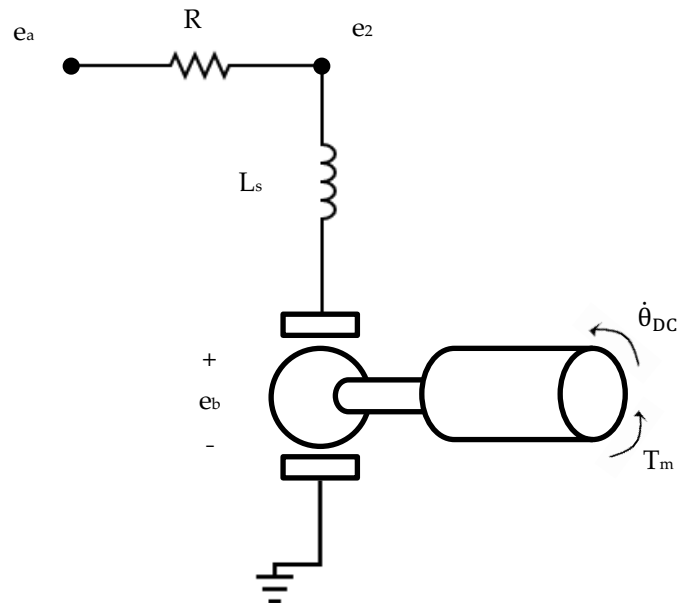


Figure 2: Modeling a DC motor with resistance and inductance

The first equation of our model relates the voltage at the positive terminal of the motor to the current through the motor. When we apply Kirchhoff's voltage law, we produce the equation

$$L \frac{di}{dt} + Ri + e_b = e_a, \quad (1)$$

which compares an input voltage e_a to the output current over time $\frac{di}{dt}$. Next, we describe the voltage source e_b , also known as a back emf. The back emf is produced as a result of the angular velocity of the motor and an emissivity constant K_e , and is described as

$$e_b = K_e \dot{\theta}_{DC}. \quad (2)$$

With the input voltage and current relation established we now form the equation

$$T_m = K_T i. \quad (3)$$

This equation relates the torque of the motor to the current through the motor and a torque constant K_T .

For the second system we take the bottom pulley attached to motor as seen in figure 2.

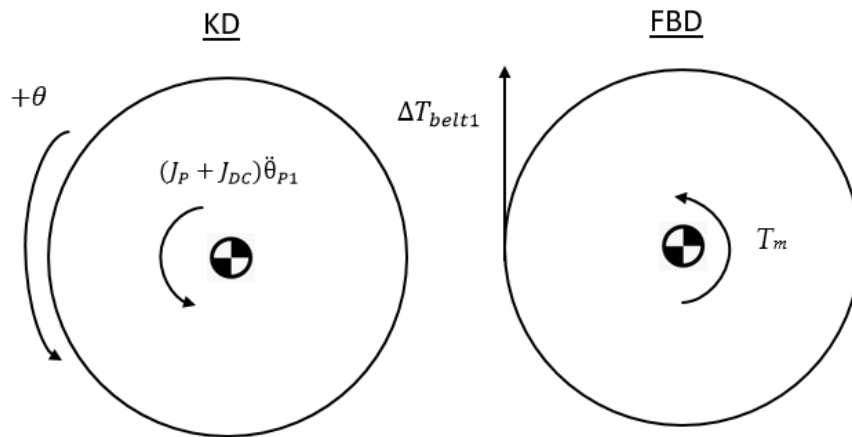


Figure 3: Kinetic and free body diagrams of the motor and pulley 1

We relate the acceleration of the motor and first pulley to the torque produced by the motor as well as the tension in the first drive belt. This produces the equation

$$(J_P + J_{DC})\ddot{\theta}_{P1} = T_m + r_{P1}\Delta T_{belt1}, \quad (4)$$

where we combine the two tensions acting on the pulley into ΔT_{belt1} to reduce the number of dependent variables. With the motion of the motor and by extension, first pulley described, we now relate the rotation of the first pulley to the second pulley. By relating the angular displacement to a linear displacement via the radius of the pulley and assuming there is no slip, we produce the equation

$$\theta_{P2} = \theta_{P1} \frac{r_{P1}}{r_{P2,1}}. \quad (5)$$

Next, we move to the second pulley in the middle as seen in figure 4 for our system.

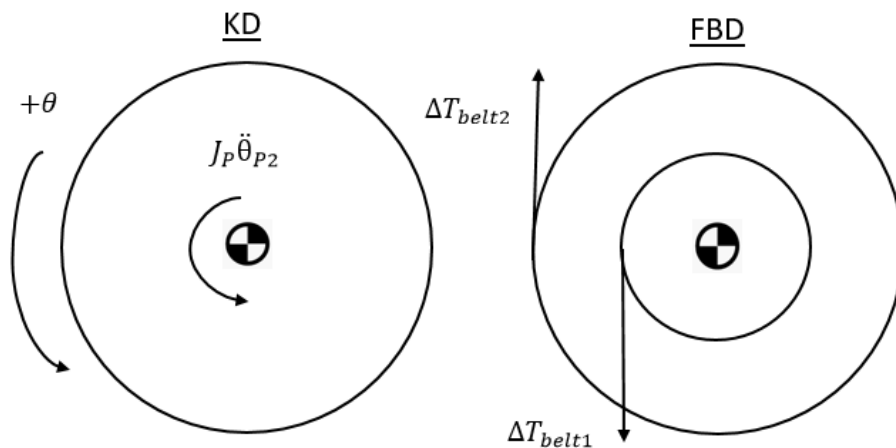


Figure 4: Kinetic and free body diagrams for pulley 2

This uses the same base equation as equation 4, relating the kinetic and free body diagrams. We have already produced the angular acceleration from equation 5 and the tension in belt 1 from equation 4, which allows us to solve for the tension in belt 2.

$$J_P \ddot{\theta}_{P2} = -r_{P2,1} \Delta T_{belt1} + r_{P2,2} \Delta T_{belt2} \quad (6)$$

We then use the top pulley as our system, as seen in figure 5.

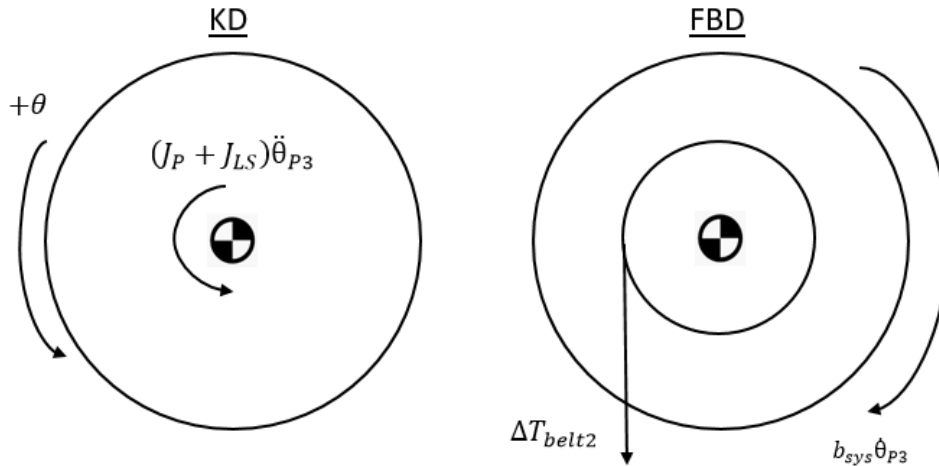


Figure 5: Kinetic and free body diagrams of pulley 3

We relate the motion of the middle pulley to that of the top pulley. This is done via the same method as equation 5, converting the angular displacement of each pulley to a linear displacement. This produces the equation

$$\theta_{P2} = \theta_{P3} \frac{r_{P3}}{r_{P2,2}}. \quad (7)$$

This relationship allows us to move to the top and final pulley. We combine the kinetic and free body diagrams to produce

$$(J_P + J_{LS}) \ddot{\theta}_{P3} = -b_{sys} \dot{\theta}_{P3} - r_{P3} \Delta T_{belt2}, \quad (8)$$

relating the movement of the pulley and leadscrew to the tension in the second belt and the friction of the bearing.

With the pulley system fully modeled, we must relate the angular displacement of the pulley to the linear displacement of the crane. To do this we take our system to be the crane as seen in figure 5.

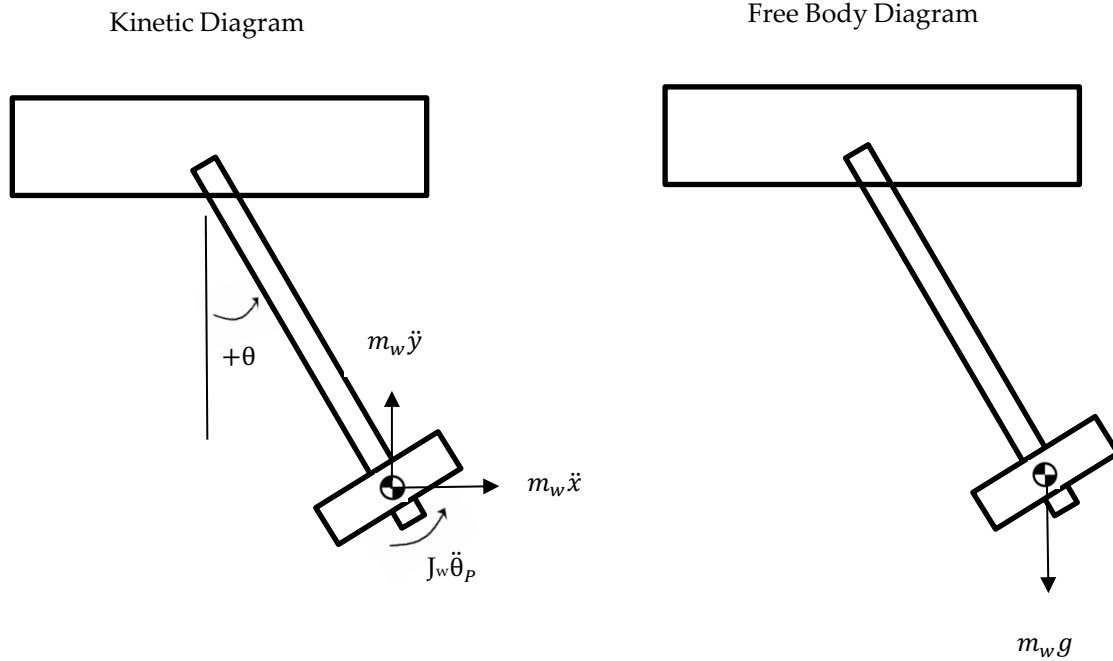


Figure 6: Modeling the crane and load

The crane is driven by a lead screw connected to pulley 3 and its displacement is a simple ratio relative to the angular displacement. From this assertion we produced

$$x_A = K_{P2}\theta_{P3}. \quad (9)$$

Next, we connect the kinetic and free body diagrams of the pendulum and crane. We assume that the mass of the crane is negligible relative to that of the pendulum and combine the systems together. This equation relates the angular momentum of the pendulum to the moment exerted on the pendulum by gravity.

$$J_w\ddot{\theta}_P + m_w\dot{y}_wL_w \sin(\theta_P) + m_w\dot{x}_wL_w \cos(\theta_P) = -m_wgL_w \sin(\theta_P) \quad (10)$$

In the x-direction, the pendulum's acceleration is composed of an angular acceleration term, an angular velocity term and the acceleration of the crane. This is represented by

$$\ddot{x}_w = \ddot{x}_A + \ddot{\theta}_P L_w \cos(\theta_P) - \dot{\theta}_P^2 L_w \sin(\theta_P). \quad (11)$$

We then find the vertical acceleration of the pendulum by applying conservation of linear momentum yielding,

$$\ddot{y}_w = \ddot{\theta}_p L_w \sin(\theta_p) + \dot{\theta}_p^2 L_w \cos(\theta_p). \quad (12)$$

To find the angular acceleration of the pendulum, we apply conservation of angular momentum to the pendulum system, which gives us

$$\ddot{\theta}_p = -\frac{L_w m_w (\cos(\theta_p) K_{P2} \theta_{P3, \dot{\dot{a}}\dot{a}} + \sin(\theta_p) g)}{L_w^2 m_w + J_w}. \quad (13)$$

To find the angular displacement of the top pulley we apply conservation of angular momentum to the system which yields

$$\ddot{\theta}_{P3} = \frac{(ic K_T r_{P2,1} r_{P3} - b_{sys} r_{P1} r_{P2,2} \dot{\theta}_{P3}) r_{P1} r_{P2,2}}{J_{DC} r_{P2,1}^2 r_{P3}^2 + J_P r_{P1}^2 r_{P2,2}^2 + J_P r_{P1}^2 r_{P3}^2 + J_P r_{P2,1}^2 r_{P3}^2}. \quad (14)$$

Finally, we find the current entering the system by applying Kirchhoff's current law to get,

$$\frac{di}{dt} = -\frac{Ri r_{P1} r_{P2,2} + K_e r_{P2,1} r_{P3} \dot{\theta}_{P3} - e_a r_{P1} r_{P2,2}}{r_{P1} r_{P2,2} Li}. \quad (15)$$

Linear Model for Design

We take the Laplace transform of equations 1-15 from the modeling section. We also apply the small angle approximation to the equations in order to eliminate non-linearities within the time-domain model. The assumptions for small angle approximation are as follows,

$$\dot{\theta}_p^2 = 0, \quad (16)$$

$$\cos\theta_p = 1, \quad (17)$$

$$\sin\theta_p = \theta_p. \quad (18)$$

We apply the small angle approximation to equation 10 from the modeling section yielding,

$$s^2 \left((L_w^2 m_w + J_w) \theta_p + L_w m_w x_A \right) = -m_w g L_w \theta_p. \quad (19)$$

We also apply the small angle approximation to the s-domain version of equation 11 and find,

$$x_w s^2 = s^2 L_w \theta_p + s^2 x_A. \quad (21)$$

Finally, the small angle approximation is applied to equation 12 in the s-domain yielding

$$y_w s^2 = \theta_p^2 s^2 L_w. \quad (22)$$

Parameter Estimation

In order to find the parameters of the DC motor, we perform some tests. We use an LCR meter on the DC motor to find

$$L_c = 1.015 \text{ mH}, \quad (23)$$

$$R = 1.9 \ \Omega. \quad (24)$$

We know the gear ratio of the gear-motor, which allows us to find the torque at the output shaft

$$T_s = 32 T_m. \quad (25)$$

We use a dynamometer to measure current and shaft torque at different values. Using this information, we used the slope of the trendline to give us

$$K_T = 2.63 \times 10^{-2} \text{ Nm/A} \quad (26)$$

$$K_V = 2.63 \times 10^{-2} \text{ V/(r/s)} \quad (27)$$

In order to determine the different parameters of our system, we use a combination of a ruler, dial caliper, and a mass balance to measure the parameters. A table with these measured values as well as calculated mass moments of inertia is shown below. The mass moment of inertia for the DC motor (J_{DC}) was estimated using spec sheets of similar sized motors.

Table 1- Recorded Parameters

Measurement	Symbol	Value	Units
Mass moment of inertia of individual pulley	J_p	0.0000812	Nm/(rad/s ²)
Diameter of small pulley	$r_{2,1}, r_3$	0.0154432	m
Diameter of large pulley	$r_1, r_{2,2}$	0.0400685	m
Mass of load	m_w	1.017	kg
Mass moment of inertia of load	J_w	0.323955553	Nm/(rad/s ²)
Length from crane to load center	L_w	0.504785	m
Mass of crane	m_c	0.583	kg
Coefficient of pitch of ball screw	K_{P2}	0.0012758	m/rad
System dampening coefficient	b_{sys}	0.00065	Nm/(rad/s)
Mass moment of inertia of the DC motor	J_{DC}	$1.4 \cdot 10^{-6}$	Nm/(rad/s ²)
Motor inductance	L_c	1.015	mH
Motor resistance	R	1.9	ohms
Proportional gain from motor input current to motor torque.	K_T	$2.63 \cdot 10^{-2}$	Nm/A
Proportional gain from motor angular velocity to back emf.	K_V	$2.63 \cdot 10^{-2}$	V/(rad/s)

Results and Discussion

Using the set of linear equations in the s-domain, we solve for the transfer function of the top pulley with the input voltage e_a as,

$$\frac{\theta_{P3}}{e_a} = \frac{r_{P1}^2 K_T r_{P3}^2}{(J_P L_c r_{P1}^4 + J_P L_c r_{P1}^2 r_{P3}^2) s^3 + (R J_P r_{P1}^4 + R J_P r_{P1}^2 r_{P3}^2) s^2 + R b_{sys} r_{P1}^4 s} \quad (28)$$

The transfer function for the angular displacement of the pendulum over the input voltage can be found as,

$$\begin{aligned} \frac{\theta_P}{e_a} = & -(s K_{P2} L_w m_w K_T r_{P3}^2) / (J_P L_c (r_{P1}^2 + r_{P3}^2) (L_w^2 m_w + J_w) s^4 \\ & + J_P R ((L_w^2 m_w + J_w) r_{P1}^2 + r_{P3}^2 J_w) s^3 \\ & + R r_{P1}^2 b_{sys} (L_w^2 m_w + J_w) s^2 \\ & + R g J_P L_w m_w (r_{P1}^2 + r_{P3}^2) s + R g L_w b_{sys} m_w r_{P1}^2). \end{aligned} \quad (29)$$

We find the transfer function of the pendulum's angular position over the input voltage to be,

$$\frac{\theta_P}{e_a} = \frac{K_{P2} r_{P1}^2 K_T r_{P3}^2}{(L J_P r_{P1}^4 + L J_P r_{P1}^2 r_{P3}^2) s^3 + (R J_P r_{P1}^4 + R J_P r_{P1}^2 r_{P3}^2) s^2 + R b_{sys} r_{P1}^4 s} \quad (30)$$

Finally, we solve for the transfer function of the crane's horizontal position x over input voltage to be,

$$\frac{x_w}{e_a} = ((gL_w m_w + s^2 J_w) K_{P2} K_T r_{P3}^2) / (s (J_P L_c (r_{P1}^2 + r_{P3}^2) (L_w^2 m_w + J_w) s^4 + J_P R ((L_w^2 m_w + J_w) r_{P1}^2 + r_{P3}^2 J_w) s^3 + R r_{P1}^2 b_{sys} (L_w^2 m_w + J_w) s^2 + R g J_P L_w m_w (r_{P1}^2 + r_{P3}^2) s + R g L_w b_{sys} m_w r_{P1}^2)). \quad (31)$$

We calculated the poles of the transfer function relating horizontal position of the load to the input voltage, equation 19, using our measured and estimated parameters. We found the dominant pole to be the complex number with a real part of -0.0337 and an imaginary part of 2.95. Using this pole, we can find the settling time of the 188.8 seconds, a peak time 1.06 seconds, and an overshoot of 96.5%. This shows that the current parameters of the system are not efficient do not allow for efficient movement of the cart with a certain input voltage. However, this can be improved with modifying the physical parameters that contribute to the denominator of equation 19. To improve this efficiency, we would need to manipulate these physical parameters to find a dominant pole with a larger real part.

Table 2 - Model Pole Information

Description	Variable	Value
Dominant pole	$s_{1,2}$	$-0.0337 \pm 2.95 j$
Settling Time	t_s	188.8 s
Peak overshoot	M_p	96.5%
Time to peak	t_p	1.06 s

When we run the simulation, we would expect the simulation to closely match experimental results. For example, if we were to plot the simulated angular velocity of the top pulley over time, we would expect the graph to quickly accelerate to a constant value when voltage input is applied. When we performed the experimental test to determine the angular velocity of the top pulley, the values for the 12V and 18V inputs were 330 rpm and 536 rpm, respectively. The resulting angular velocities over time for the model simulation are plotted below.

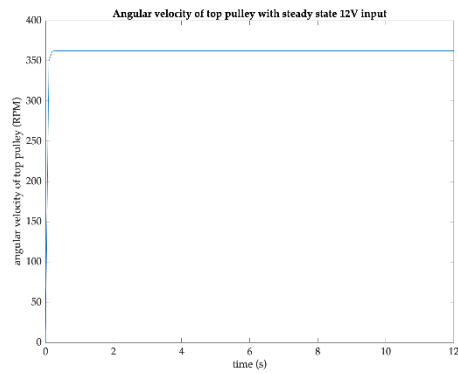


Figure 7: Simulation results for angular velocity of top pulley vs. time with 12V input

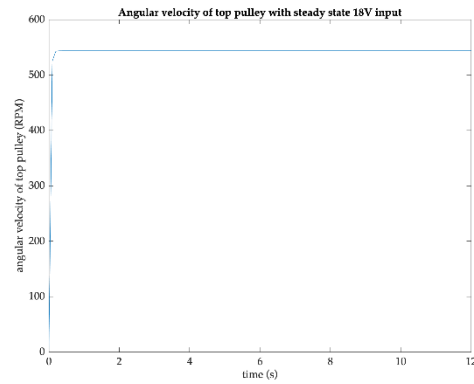


Figure 8: Simulation results for angular velocity of top pulley vs. time with 18V input

The constant angular acceleration values of the top pulley for the 12V and 18V inputs are 358 rpm and 536 rpm, respectively. These values match the experimental values closely which gives us confidence that our model accurately predicts the behavior of the physical system.

When we run the physical system and monitor the swing of the pendulum and load, we notice that as the crane reaches the end of the track it is on and begins to move in the other direction, the load swings significantly more than it did before changing directions. The sudden change in momentum of the crane in one direction to the other direction creates this sporadic swing in the load. We would expect a similar phenomenon to occur in our model simulation. The plot below shows the vertical position vs. the horizontal position of the load during the simulation. The blue line on the plot indicates the vertical position of the load on the way down the track while the red line indicates the vertical position of the load on the way back to the beginning after reaching the end of the track.

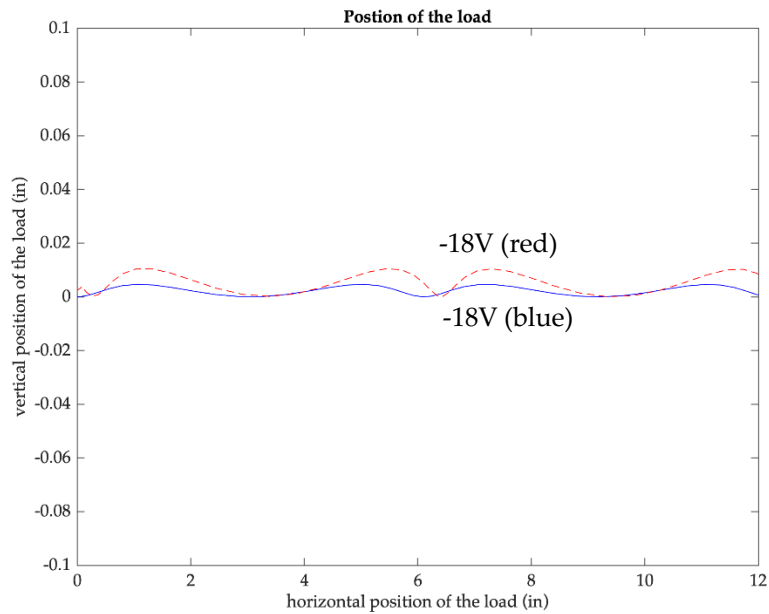


Figure 9: Simulation results for vertical position of load vs. horizontal position of the load

The plot of the simulated vertical position of the load tells us that there was not very much vertical movement on the way down the track, but as the crane reached the end and began moving back towards the beginning, there was more vertical movement in the load. This is shown by the taller peaks in the red line in comparison to the blue line. This indicates that the load reached greater heights on the trip back to the beginning than it did on the way towards the end of the track.

When running the physical system, we see that the angular velocity of the top pulley spins the lead screw and moves the crane. We know that the top pulley spins at a constant rate after quickly accelerating to this constant rate. As the crane movement is dependent on the angular velocity of the top pulley, we would expect the crane to move at a constant linear velocity. In order to check that our model correctly predicts the movement of the crane, we simulated the model and plotted the horizontal displacement of the crane over time below.

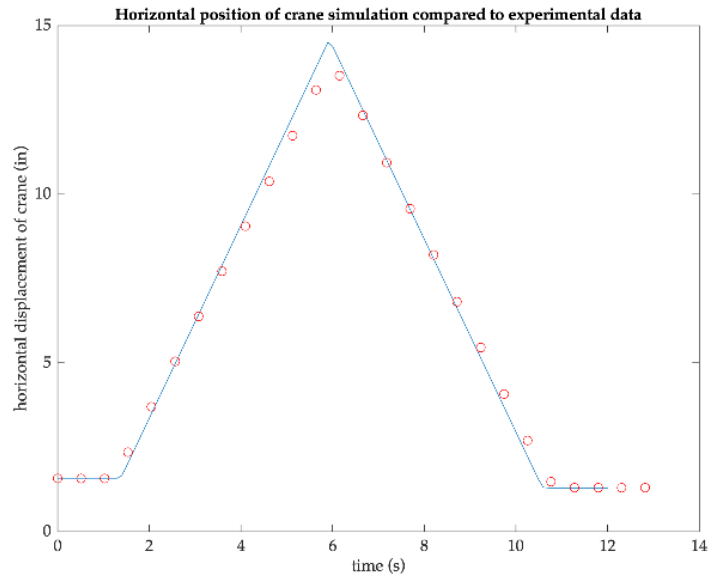


Figure 10: Simulation results for horizontal displacement of the crane vs. time

As we would expect, our model simulation of the horizontal displacement of the crane over time increases as it moves outwards away from the starting position and decreases as it moves back towards the starting position. The rate at which the crane moves is constant as well which is what we would expect because the crane's movement is reliant on the constant angular velocity of the top pulley.

Another aspect of the physical system we would expect is that the input voltage would produce a certain constant angular velocity of the top pulley in the system. We would expect to see different angular velocities for different input voltages. When we run the model simulation and plot the angular velocity of the top pulley for 12 seconds, we obtain the graph shown below.

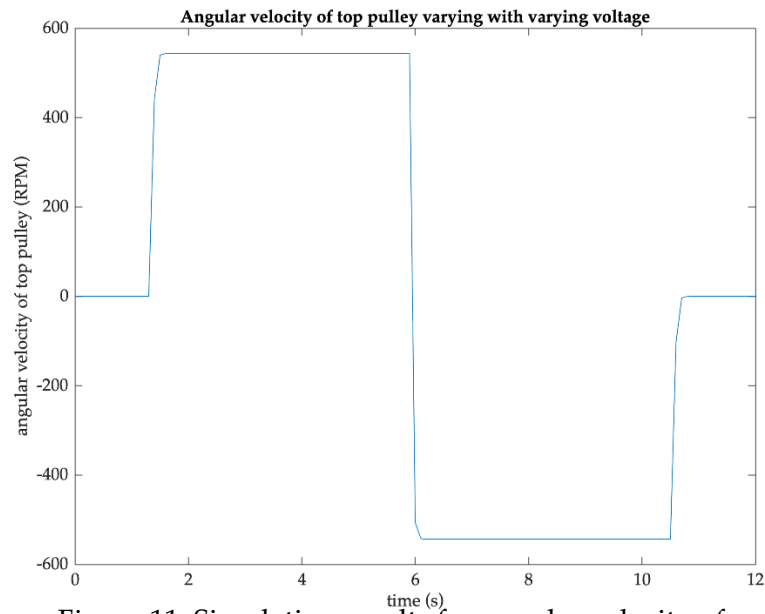


Figure 11: Simulation results for angular velocity of top pulley based on input voltage

The graph shows that when a positive 18V input voltage is applied at around 2 seconds, the angular velocity of the top pulley sharply increases to a constant value of 536 rpm. This value matches the value we determined earlier for an 18V input. Moreover, when the input voltage is switched to negative 18V at 6 seconds, the angular velocity quickly changes to -536 rpm. This is what we would expect to happen since the magnitude of the input voltage is the same, but a negative voltage would change the direction of rotation of the top pulley.

Conclusion

The model created can accurately predict the behavior of a gantry crane system. In this paper we created a transfer function to model the behavior of a crane and load system. We achieved this by modeling the individual components of the system and creating a transfer function relating the voltage input to the angular displacement of the pendulum over time. Our model accuracy by comparing the angular velocity of the top pulley over time with the input voltage. This produced results of 358 RPM at 12 volts and 536 RPM at 18 volts. These values matched the experimentally determined values of 330 RPM at 12 volts and 536 RPM at 18 volts. We also measured linear displacement of the crane, and the model accurately described the experimental behavior of the system. The plot of crane position also matched our prediction of how a crane would behave. The results of the simulation align closely with the experimentally determined data. Our model may be used to create a control circuit to adjust the behavior of the suspended load.